

The Influence of Surface Roughness and Piezo-Viscous Lubricant Properties on the Elastohydrodynamic Line Contact Lubrication

V. D'Agostino^{1,2}, V. Petrone² and A. Senatore^{1,2}

¹Department of Industrial Engineering, University of Salerno, Italy

²Nano_Mates, Research Centre for Nanomaterials and Nanotechnology at Salerno University, Italy

Abstract

In this paper a numerical solution of the elastohydrodynamic line (EHL) contact lubrication problem is presented for a cylinder which is rolling over a flat plane. As is well known, the properties of the lubricant play a significant role in the forming of a lubricating film and reducing friction between the contacting surfaces. Pressure profiles and film shapes are shown and variations of the minimum film thickness with dimensionless parameters are also presented. The influence of pressure and temperature on viscosity, limiting shear stress and density, has been taken into account when lubricant models have to be used in numerical calculation of film thickness and friction. The effects of different pressure–viscosity relationships, including the exponential model, the Roelands model and the free-volume model, are investigated on modelling in the best possible way the real piezo-viscous behaviour at pressures as high as the typical EHL pressures.

The role of surface roughness on EHD lubrication has become crucial, for this reason its effect on the pressure profile and film thickness in a steady state EHL line contact is, also, investigated by means of numerical simulations. One of the purposes of this work, in fact, is to show how the pressure profile and film thickness are influenced by surface asperity, not only by modelling the roughness using deterministic or averaging techniques, but by introducing a real surface topography of the contact surfaces. The roughness data of a real surface has been collected using a three-dimensional no-contact profilometer based on confocal microscopy technology.

Keywords: elastohydrodynamic line, roughness, piezo-viscosity, free volume, Reynolds equation; film thickness.

1 Introduction

A good and accurate prediction of the elastohydrodynamic lubrication (EHL) behaviour requires the resolution of the constitutive equations for lubricated

contacts. The EHL has two primary aspects: the strong increase of viscosity with pressure, and the magnitude of the elastic deformation caused by high pressure which is comparable to that of the film thickness. Due to the high pressure and the limited contact area elastic deformation of the surfaces will occur and it is not negligible, as well as the pressure dependence of viscosity play a crucial role in EHL simulation because the viscosity at the inlet has crucial influence on film formation. The rheology of liquid lubricants in the Hertzian zone of concentrated contacts has been of principal interest to tribologists many years. In particular, for applications involving lubricants that exhibit shear-thinning behaviour, the use of an appropriate non-Newtonian fluid model is required to predict the EHL behaviour more accurately. For this reason, this paper aims to emphasize the importance of implementing realistic non-Newtonian and piezo-viscous models with accurate treatment methods in EHL applications.

The exponential [1] and Roelands [2] equations are widely used to describe the pressure-viscosity relationship in EHL simulations. However, the real responses of most lubricants are often non-linear [3]. It is usually difficult to predict the non-linearity accurately by the exponential equation, and the value is likely to be underestimated by the Roelands equation [4].

In the light of the above facts, in order to a better modelling of the lubricant rheology Doolittle [5] developed the first free-volume model based on a physical meaning, that the resistance to flow in a liquid depends upon the relative volume of molecules present per unit of free volume. Using an exponential function, Doolittle related viscosity to the fractional free volume. The Williams–Landel–Ferry (WLF) equation [6] can be derived from the Doolittle free-volume equation; this one, subsequently improved by Yanutsomi [7] and Cook [8], may accurately describe the temperature variation of viscosity and, above all, obtain an accurate description of viscosity variation with pressure.

In this paper the effects of different pressure–viscosity relationships on film thickness, including the Barus model, the Roelands model, and the free-volume model, are investigated through a numerical simulation taking into account the physical characteristics of the lubricant.

At the same time, the conditions under which lubricated contacts in machine element applications have to operate reliably have become much more severe in the past years. As a result the nominal film thickness in the contacts has decreased to a level where the influence of surface roughness becomes significant. This issue has focused the attention of the researchers on the study of the influence of surface texture in elastohydrodynamic lubrication especially on the elastic deformation of the roughness inside the contact.

The studies on roughness deformation have produced a lot of knowledge on how roughness and its effect can best be characterized for prediction purposes. In particular the approach based on single harmonic components, developed by Venner and Lubrecht [9] Masen et al. [10] has also proven to be partially useful. The purpose of this paper is to study systematically the effect of longitudinal roughness on friction by means of numerical simulations, for this reason, it has been shown how the pressure profile and film thickness are influenced by surface asperity, not only by modelling the roughness using deterministic or averaging techniques, but by

introducing a real surface topography of the contact surfaces. For this reason, three types of surfaces are employed for cases in line contacts. Firstly the classical smooth profile; a second case in which the surface roughness is assumed to be transverse and its profile is generated by a sinusoidal function defined in terms of its amplitude and wavelength. Subsequently, in the third analysed case was considered the topography of a rough surface and its orientation. The roughness data of a real surface has been collected through a 3D no-contact profilometer based on confocal microscopy technology because confocal profiling provides the highest lateral resolution that can be achieved by an optical profiler.

2 Numerical results

2.1 Governing equations

The classical EHL problem consists of principally three equations that have to be solved simultaneously. These are the Reynolds equation, the film thickness equation including the elastic deformation and the force-balance equation. The desired outputs related to the resolution of this system are, usually, the pressure distribution and the film thickness variation. In addition to these three equations, the density and viscosity-pressure relations have to be calculated inside the lubricated meatus (see Appendix).

Reynolds Equation. According to isothermal EHL theory, the film profile and pressure distribution in line EHL contacts are expressed by the equivalent elastic modulus E' , equivalent radii in the x direction R , properties of lubricant, average velocity u_m and the applied load w . The classical Reynolds equation for the case of smooth surfaces is:

$$\frac{\partial}{\partial x} \left(\frac{\rho h^3}{\eta} \frac{\partial p}{\partial x} \right) - 6 \frac{\partial}{\partial x} (u_m \rho h) = 0$$

where $u_m = \frac{U_1 + U_2}{2}$, U_1 and U_2 are the surface velocities and in this analysis no slip condition has been supposed so that the surface velocities are identical to the lubricant velocities.

The boundary conditions are $p=0$ at the boundaries of the calculational domain and the cavitation condition is $p = 0$ at the cavitation boundary.

Film Thickness Equation. The film thickness equation, describing the distance between the two contacting surfaces, consists of two components, the gap between the undeformed surfaces and the elastic deformation of the surfaces. Consequently, the gap between the elastically deformed surfaces, generally described by the film thickness equation, is calculated in each point of the x direction as:

$$h(x) = h_0 + \frac{x^2}{2R} - \frac{4}{\pi E'} \int_{-\infty}^{+\infty} p(x') \ln \left(\frac{|x - x'|}{b} \right) dx'$$

Force Balance Equation. An equation is also needed to make sure that the load and the pressure in the contact are in equilibrium. This equation is usually called the force balance equation. In full film conditions, the load per width unit is carried by the lubricant film and the calculation is an integration of the lubricant film pressure.

$$w = \int_{-\infty}^{+\infty} p(x) dx$$

In conjunction with these three equations, a density model has been used for these EHL simulations. Due to the isothermal conditions assumed in this work, the density model used is only pressure dependent and it has been developed by Dowson and Higginson [11], in which a model for the relation between the density and the pressure for a lubricant is presented.

$$\rho(p) = \rho_0 \frac{5.9 \cdot 10^8 + 1.34 p}{5.9 \cdot 10^8 + p}$$

2.2 Viscosity model

An important factor which plays a decisive role in the prediction of film thickness and pressure distribution is the piezo-viscous response of lubricants.

2.2.1 Barus and Roelands models

The majority of available studies on EHL contacts often use one of the two well-known pressure-viscosity equations given below:

Barus model:

$$\mu = \mu_0 \exp(\alpha \cdot p)$$

Roelands model:

$$\mu = \mu_0 \exp \left[(\ln \mu_0 + 9.67) \left(-1 + \left(1 + 5.1 \cdot 10^{-9} p \right)^z \right) \right]$$

particularized with $z=0.6$ (Fig. 1).

Dimensionless pressure profiles and film shapes variations with dimensionless load and sliding speed parameters in a domain $-1.5 < X < 1.5$ are presented in the Figs.2-3. The model predicts that a pressure spike occurs on the outlet side of the contact, accompanied by a constriction in oil-film thickness. Increasing speed or decreasing applied load causes the increasing of the pressure spike in height and its moving from the outlet side of the contact toward the inlet.

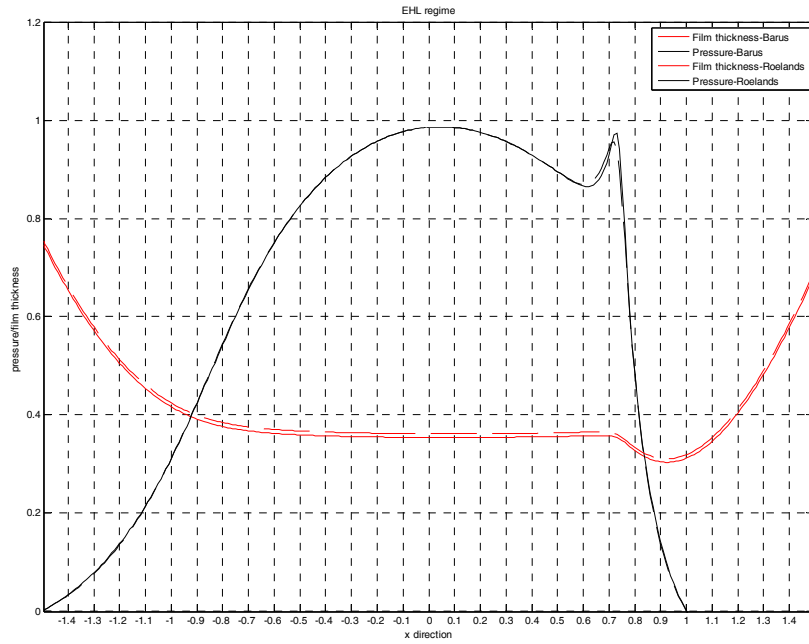


Figure 1: Film thickness profile and pressure distribution using Roleands law (solid line) and Barus law (dashed line) with $W=3.0 \times 10^{-4}$; $U=2.0 \times 10^{-11}$.

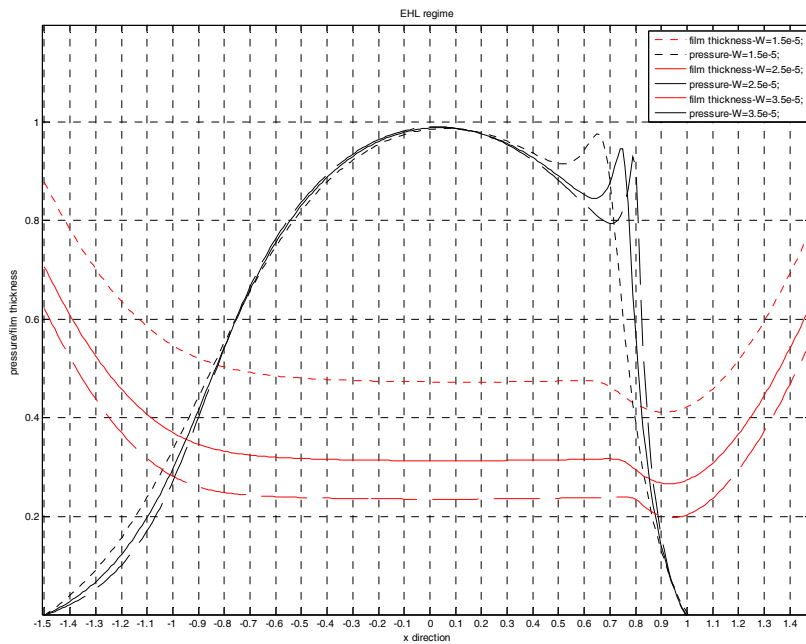


Figure 2: Film thickness profile and pressure distribution comparison using Roelands law, with $W=1.5 \times 10^{-4}$ (dot line); $W=2.5 \times 10^{-4}$ (solid line), $W=3.5 \times 10^{-4}$ (dashed line)

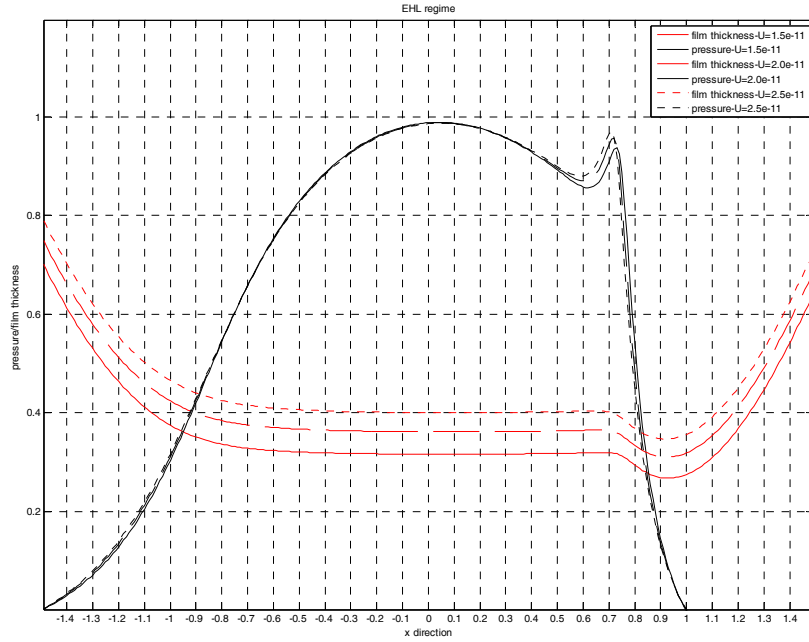


Figure 3: Film thickness profile and pressure distribution comparison using Roelands law, with $U=1.5 \times 10^{-11}$ (solid line); $U=2.0 \times 10^{-11}$ (dashed line), $U=2.5 \times 10^{-11}$ (dot line)

On the other side, for the film thickness behaviour, increasing the dimensionless sliding speed, the height of the meatus increases, while for an increase in applied load a reduction of the film thickness is observed.

These results are due to a progressive variation of the lubrication regime as a function of speed and applied load parameters. In fact an increase of the load causes a progressive predominance of the boundary lubrication regime condition, while increasing the sliding speed hydrodynamic lubrication regime is expected with a higher fluid meatus. This result is well described in the Stribeck curve [12] in which the coefficient of friction is usually represented as a function of a dimensionless lubrication parameter $\eta v/P$, where η is the dynamic viscosity, v the sliding speed and P the load projected on to the geometrical surface dimensionless per unit length. For smaller values of the Stribeck parameter, e.g. due to an increase of the load, boundary lubrication is the major lubrication regime, while an increase in this parameter, e.g. an increase in the sliding speed, causes a displacement towards the hydrodynamic lubrication region.

In the recent years, the crucial focus on the real pressure-viscosity relationship is that neither of the above two equations successfully model the real piezo-viscous behaviour at pressure as high as the typical EHL pressure.

For this reason it was necessary using a more accurately model such as the free-volume viscosity model.

2.2.2 Free-volume model

Doolittle [5] developed the first free-volume model based on a physical meaning, that the resistance to flow in a liquid depends upon the relative volume of molecules present per unit of free volume. The free volume of a liquid was originally considered to be the volume resulting from the thermal expansion without phase change. Using an exponential function, Doolittle related viscosity to the fractional free volume. In this work, the Doolittle's viscosity–pressure relationship is represented by :

$$\mu = \mu_0 \exp \left(B \frac{V_\infty}{V_0} \left[\frac{1}{\frac{V}{V_0} - \frac{V_\infty}{V_0}} - \frac{1}{1 - \frac{V_\infty}{V_0}} \right] \right)$$

Where B and $\frac{V_\infty}{V_0}$ are constants and $\frac{V}{V_0}$ can be calculated using the Tait's equation [13,14]:

$$\frac{V}{V_0} = 1 - \frac{1}{1 + K'_0} \ln \left[1 + \frac{p}{K_0} (1 + K'_0) \right]$$

The lubricant in the proposed model is characterized by $\mu_0 = 1.3 \text{ Pa}\cdot\text{s}$; $B = 4.422$;

$$\frac{V_\infty}{V_0} = 0.6694; K'_0 = 12.83, K_0 = 1.4252 \text{ GPa} [15].$$

Fig.4 shows the pressure distribution and film thickness profile obtained from a static load EHL analysis with the free-volume model. The dimensionless load is $W = 3.0 \times 10^{-4}$, the dimensionless sliding speed is $U = 2.0 \times 10^{-11}$ and the dimensionless material parameter is $G = 4000$. The maximum Hertzian contact pressure, for this operating conditions, p_h , is 1.25 GPa.

A behaviour similar to those reported previously using the Roelands law, for the pressure distribution and film shape, in function of the dimensionless applied load and sliding speed, has been observed with the use of the free-volume model. In fact an increase in sliding speed or a decrease in applied load causes the increasing of the pressure spike in height and its moving from the outlet side of the contact toward the inlet (Fig.5).

In particular in the figures below are also shown the graphs of viscosity as a function of different levels of applied load (Fig.6) and sliding speed (Fig.7).

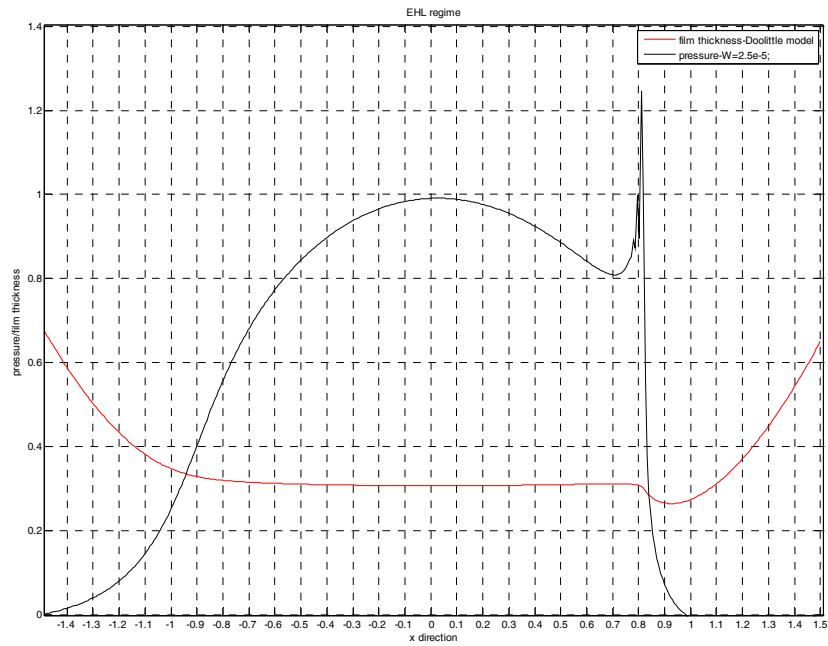


Figure 4: Figure 1: Film thickness profile and pressure distribution using Doolittle model with $W=3.0 \times 10^{-4}$; $U=2.0 \times 10^{-11}$.

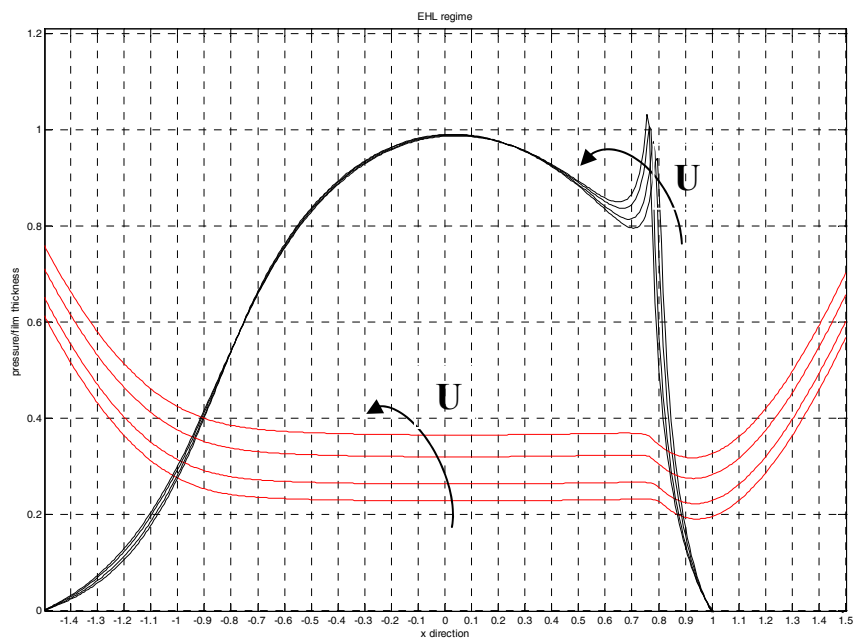


Figure 5: Film thickness profile (red line) and pressure distribution (black line) comparison using Doolittle model for different level of dimensionless sliding speed (from $U=1.0 \times 10^{-11}$ to $U=6.0 \times 10^{-11}$)

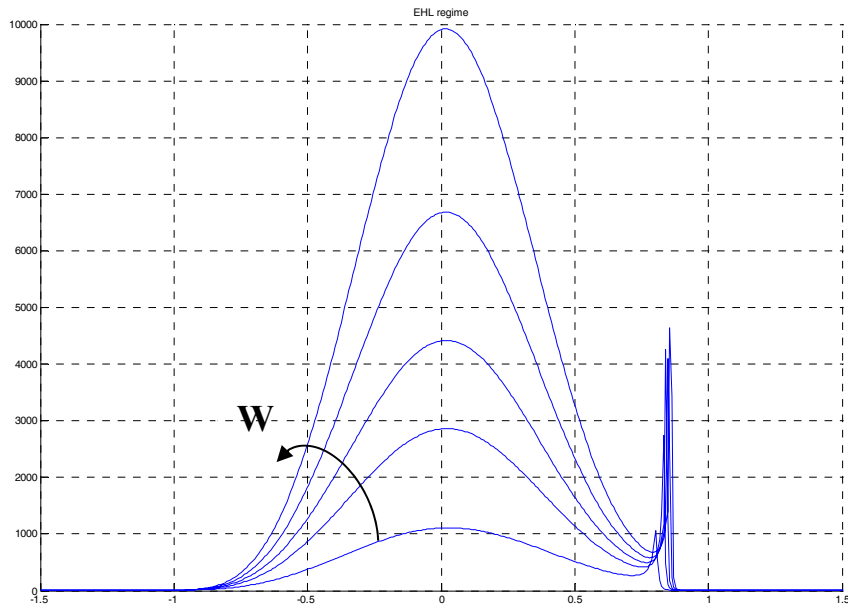


Figure 6: Viscosity distribution comparison using Doolittle model for different level of dimensionless applied load (from $W=1.0 \times 10^{-4}$ to $W=6.0 \times 10^{-4}$)

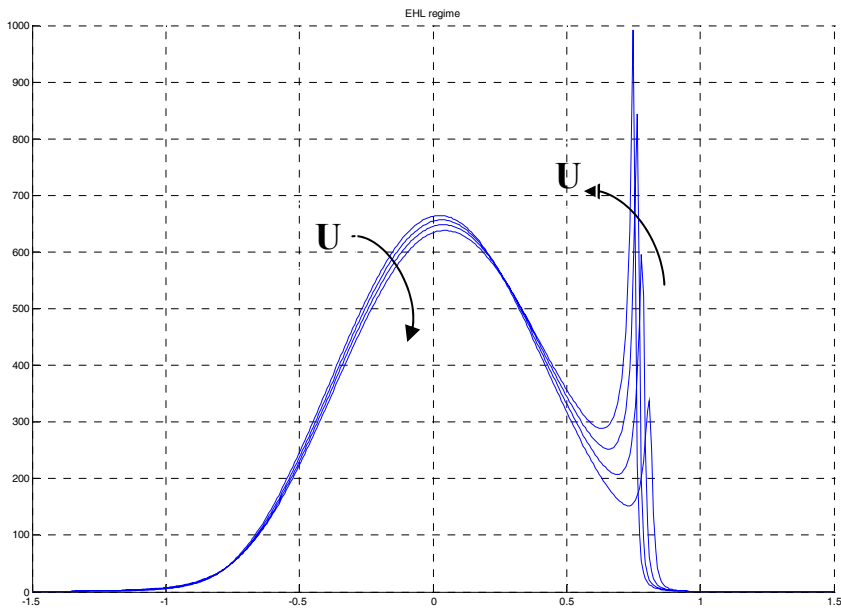


Figure 7: Viscosity distribution comparison using Doolittle model for different level of dimensionless sliding speed (from $U=1.0 \times 10^{-11}$ to $U=6.0 \times 10^{-11}$)

Comparing the results obtained, in terms of pressure distribution and film thickness, using the free-volume model and the Roelands one for the viscosity-pressure relationship, it is possible to observe a pressure spike amplitude of about 25% higher using the model based on the free-volume theory (Fig.8).

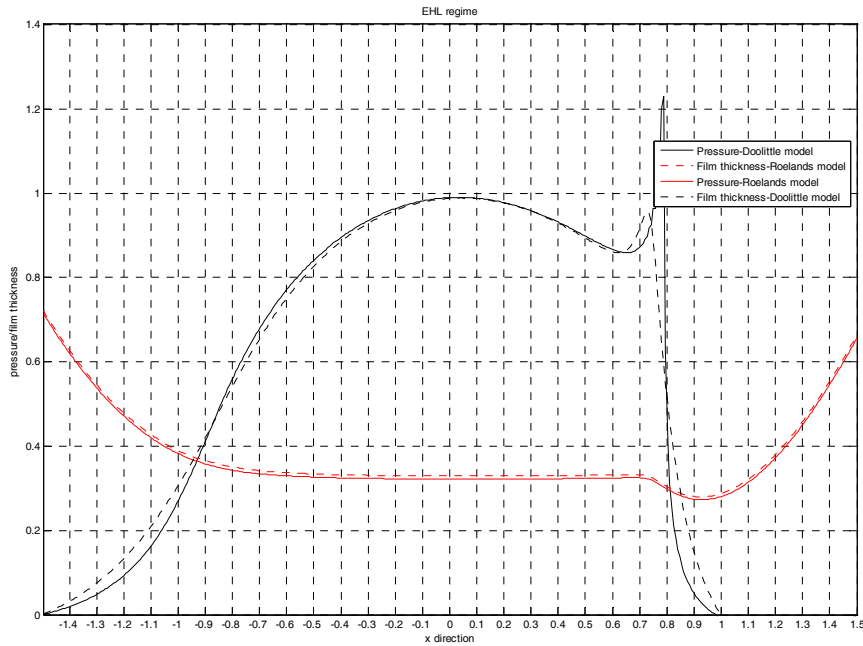


Figure 8: Film thickness profile and pressure distribution using Doolittle model (solid line) and Roelands law (dashed line) with $W=3.0 \times 10^{-4}$; $U=2.0 \times 10^{-11}$.

It is also seen that the difference in central pressure is about 2%. Similarly it can be seen that the height of the film thickness is smaller for the proposed model even if in a small percentage of about 3%. The remarkable difference as regards the pressure magnitude inside the contact area could also influence the sub surface stresses, for this reason the risk of surface fatigue can be estimated more accurately.

For many years, an important parameter of comparison with regard to the EHL lubrication is the central and the minimum value of the film thickness. Indeed, already during the 1970's, Hamrock and Dowson [16,17], presented their today well known equations for the central and minimum film thickness for hard and soft EHL. These equations already highlighted the importance of the relationship between pressure and viscosity in the calculations of the film thickness. By comparing the numerical results obtained using the two proposed viscosity models in this work it could be observed that the use of Roelands law tends to overestimate the height of the minimum and central film thickness in each considered operating conditions (Figs. 9-12).

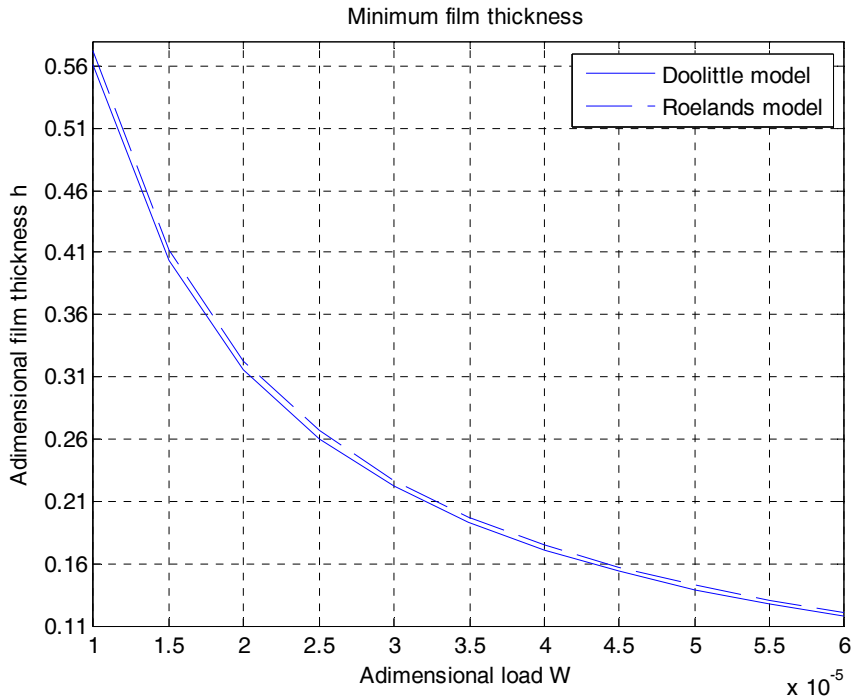


Figure 9: Minimum film thickness values comparison for different level of dimensionless applied load (from $W=1.0 \times 10^{-4}$ to $W=6.0 \times 10^{-4}$)

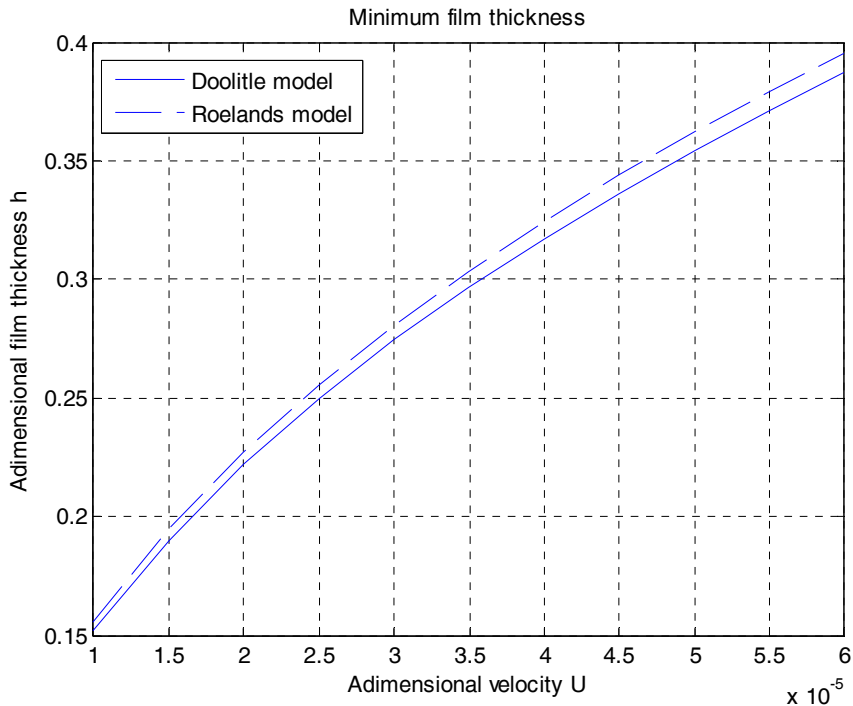


Figure 10. Minimum film thickness values comparison for different level of dimensionless sliding speed (from $U=1.0 \times 10^{-11}$ to $U=6.0 \times 10^{-11}$)

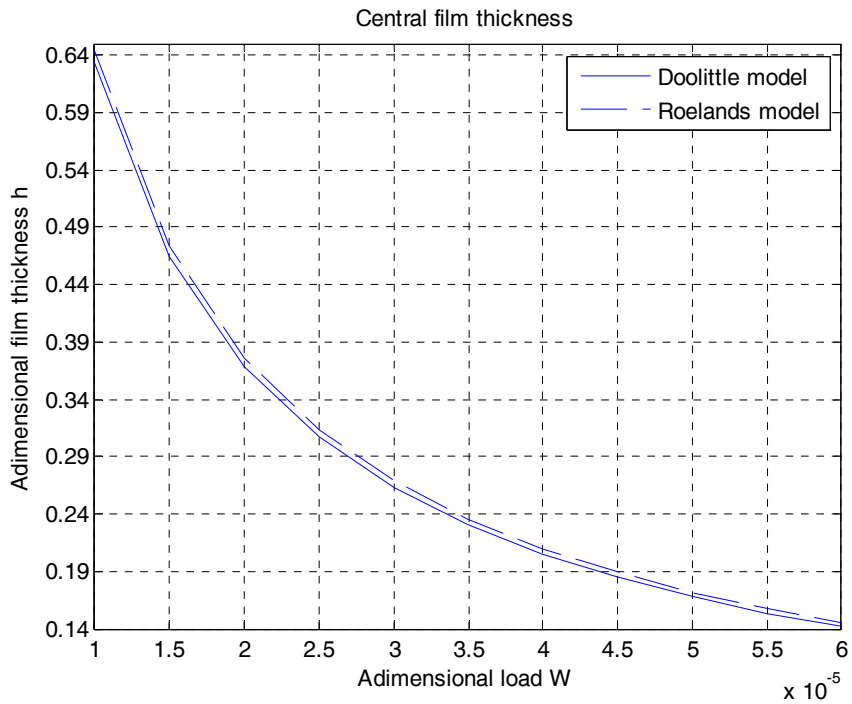


Figure 11: Central film thickness values comparison for different level of dimensionless applied load (from $W=1.0 \times 10^{-4}$ to $W=6.0 \times 10^{-4}$)

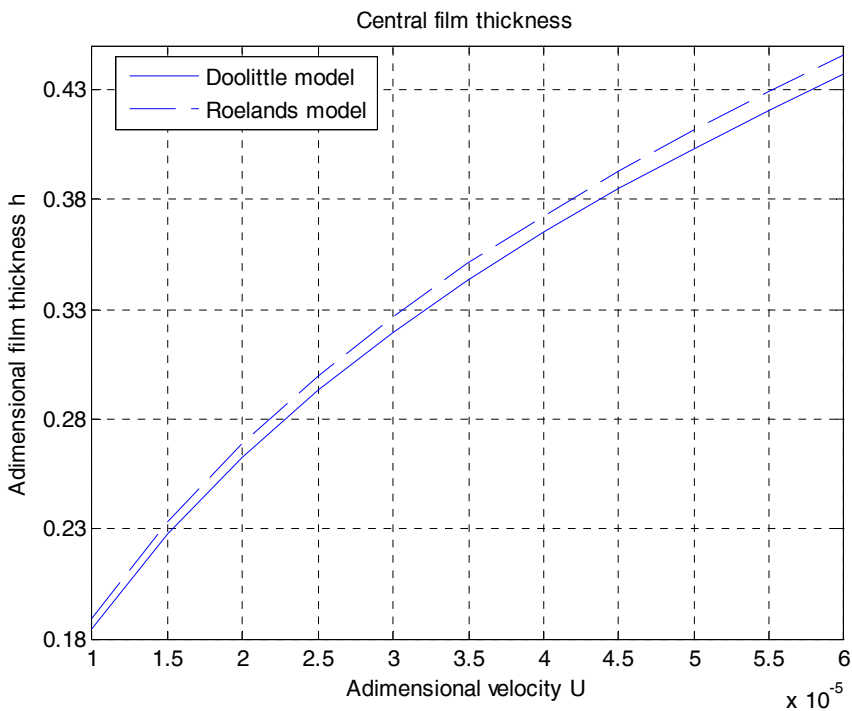


Figure 12: Central film thickness values comparison for different level of dimensionless sliding speed (from $U=1.0 \times 10^{-11}$ to $U=6.0 \times 10^{-11}$)

2.3 The effect of the roughness

The proposed model is also used in order to investigate the effect of different types of rough surface on EHL lubrication performance.

For this reason, three types of surfaces are employed for cases in line contacts. Firstly the classical smooth profile; a second case in which the surface roughness is assumed to be transverse and its profile is generated by a sinusoidal function defined in terms of its amplitude and wavelength. Subsequently, in the third analysed case the topography of a rough surface and its orientation have been considered. The roughness data of a real surface has been collected through a 3D no-contact profilometer based on confocal microscopy technology.

2.3.1 Sinusoidal wave roughness

The presence of a sinusoidal waviness on one of the contacting surfaces causes relative variations on the pressure distribution and film shape that would be obtained with perfectly smooth surfaces[18-20]. The magnitude of these variations depends on the operating conditions, the lubricant characteristics, and the roughness geometry. In particular it depends on the response of the shear stress to viscosity fluctuations caused by the pressure variations, so that the importance of the piezo-viscous behavior is also confirmed.

The numerical results are obtained considering the dimensionless parameters: $W=3.0 \times 10^{-4}$; $U=2.0 \times 10^{-11}$; $G=4000$; and the cylinder radius equal to $R=0.005$ m. The waviness is characterized by its dimensionless amplitude A and wavelength W . Regarding the amplitude it is useful to introduce another dimensionless quantity, the relative amplitude A^* defined as $A^*=5A/H_c$ where H_c is the dimensionless smooth central film thickness. The values of A considered in this work is 0.02, while for W are 150 and 15 ($\lambda=1000, 100$).

$$R(x) = A \sin \lambda x$$

where $\lambda=2\pi/W$,

As expected, the pressure distribution and the film shape exhibit sinusoidal-like variations (Fig. 13).

2.3.1 A real surface topography

Furthermore, the analysis has been extended to a real surface topography. The roughness profile has been acquired by a 3D no-contact profilometer (Sensofar PLU-Neox) based on confocal microscopy technology with two important qualities: non-invasive and high accurate measurements. In Fig.14-15 are reported the linearized roughness measured on x direction and an image of the real 3D topography.

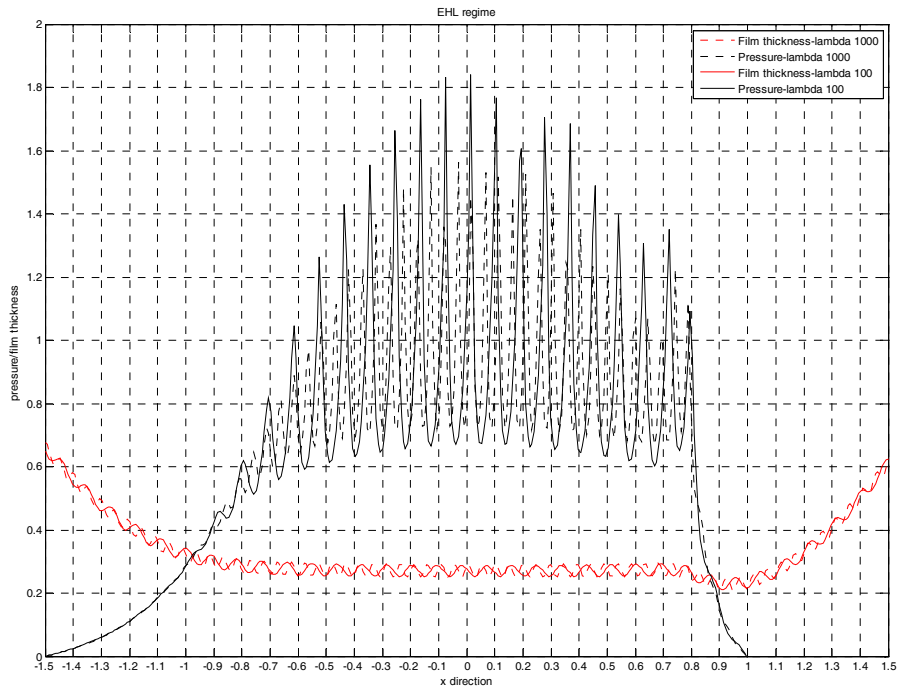


Figure 13: Film thickness profile and pressure distribution with $\lambda=1000$ (solid line) and $\lambda=100$ (dashed line).

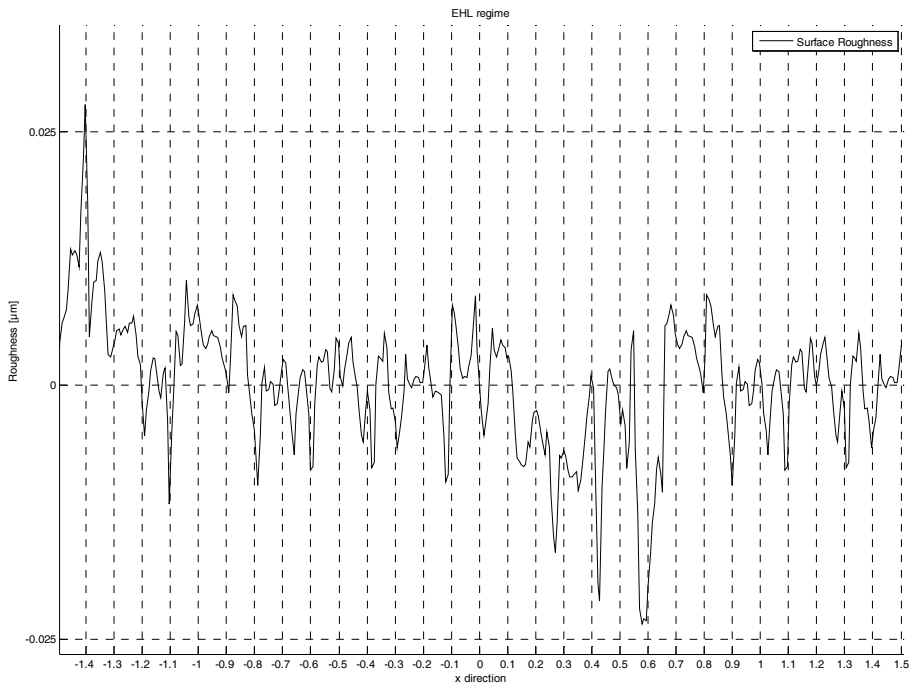


Figure 14: Real surface roughness profile in x direction

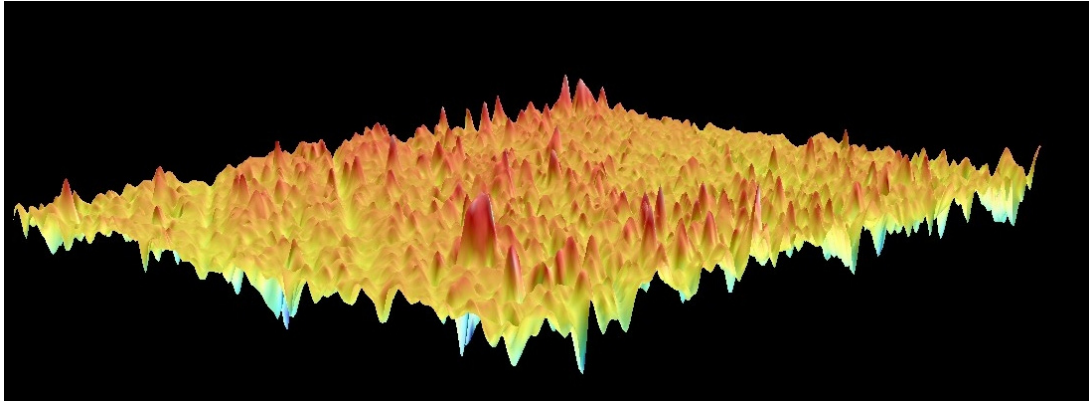


Figure 15: A particular of real surface 3D topography

The result of this simulation shows a significant pressure and film thickness fluctuations within the contact zone. The local pressure values changes drastically along the x axis with a maximum hertzian contact pressure $p_h=1.41$ GPa (Fig. 16).

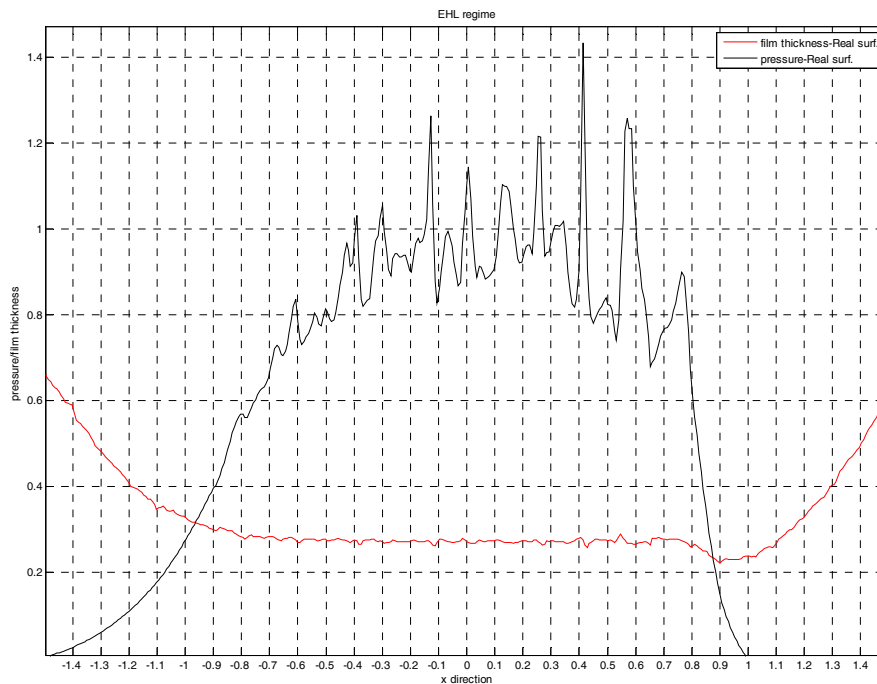


Figure 16: Film thickness profile and pressure distribution using Doolittle model and real surface roughness with $W=3.0 \times 10^{-4}$; $U=2.0 \times 10^{-11}$

The result emphasizes the importance of the measuring the real surface roughness of the materials to be able to estimate accurately the pressure values that can be reached in the contact area which strongly influence the values of the coefficient of friction and the surface fatigue of the mating materials.

3 Conclusions

In this paper numerical results in EHL line contact modelling with non-Newtonian fluids and roughness surfaces have been presented. The Roelands law, usually used for modelling the pressure-viscosity relationship of the lubricants has been observed to fail in capturing the real film thinning behaviour. For this reason, a law based on the free-volume theory model has been used to predict the EHL characteristics (pressure distribution and film thickness) over a wide range of sliding speed and applied loads with a better characterization of the shear-thinning lubricant behaviour. In fact, it was found that the film thickness becomes more thinner using the free-volume model and in particular the pressure spike magnitude increase significantly. This paper also aims to highlighted the importance of knowing the real surface topography to estimate the real values of the pressure distribution inside the contact area.

In fact, numerical simulations have shown the influence of the surface roughness on the EHL properties, for this reason an optical profilometer has been used to acquire the three-dimensional surface topography in order to evaluate the values of pressure and film thickness more accurately.

References

- [1] C. Barus, “*Isothermal, isopiestic and isometrics relative to viscosity*” Am. J. Sci. 45, 87-96, 1893.
- [2] C.J.A. Roelands, “*Correlational Aspects of the Viscosity–Temperature–Pressure Relationship of Lubricating Oils*”, PhD thesis (Delft University, Delft), 1996.
- [3] S. Bair, “*The high pressure rheology of some simple model hydrocarbons*”, Proc. Instn. Mech. Engrs. 216(J) 223, 2002.
- [4] S. Bair, “*Roelands' missing data*”, Proc. Instn. Mech. Engrs. 218(J1) 57-60, 2004.
- [5] A.D. Doolittle, “*Studies in Newtonian Flow. II. The Dependence of the Viscosity of Liquids on Free Space*”, J. Appl. Phys. 22(12) 1471, 1951.
- [6] M.L. Williams, R.F. Landel and J.D. Ferry, “*The Temperature Dependence of Relaxation Mechanisms in Amorphous Polymers and Other Glass-forming Liquids*”, J. Am. Chem. Soc. 77, 3701-3707, 1955 .
- [7] S. Yasutomi, S. Bair and W.O. Winer, “*An Application of a Free Volume Model to Lubricant Rheology I—Dependence of Viscosity on Temperature and Pressure*”, ASME J. Lubr. Techn.106(2) 291, 1984.
- [8] R.L. Cook, C.A. Herbst and H.E. King Jr, “*High-pressure viscosity of glass-forming liquids measured by the centrifugal force diamond anvil cell viscometer*”, J. Phys. Chem. 97 2355, 1993.
- [9] C. H. Venner and A. A. Lubrecht, “*Amplitude Reduction of Anisotropic Harmonic Surface Patterns in EHL Circular Contacts Under Pure Rolling*”, Proc. 25th Leeds-Lyon Symposium on Tribology, pp. 151–162, 1999

- [10] M.A Masen, C.H. Venner, P.M. Lugt, and J.H. Tripp, “*Effects of Surface Micro-Geometry on the Lift-Off Speed of an EHL Contact*”, Tribol. Trans., 45, pp. 21–30, 2002.
- [11] D. Dowson and G. R. Higginson, “*Elastohydrodynamic Lubrication, The Fundamentals of Roller and Gear Lubrication*”, Pergamon Press, Oxford, 1966
- [12] Xiaobin Lu, M. M. Khonsari, and E. R. M. Gelinck, “*The Stribeck Curve: Experimental Results and Theoretical Prediction*”, J. Tribol. 128, 789, 2006.
- [13] Y. Liu, Q.J. Wang, W. Wang, Y. Hu, D. Zhu, I. Krupka *et al.*, “*EHL simulation using the free-volume viscosity model*”, Tribol Lett, 23, 1, pp. 27–37, 2006.
- [14] S. Bair, “*High pressure rheology for quantitative elastohydrodynamics*”, tribology and interface engineering series no. 54 Elsevier, Amsterdam, Netherland, 2007.
- [15] Y. Liu, Q.J. Wang, S. Bair, P. Vergne, “*A quantitative solution for the full shear-thinning EHL point contact problem including traction*”, Tribol Lett, 28, 2, pp. 171–181, 2007.
- [16] B.J. Hamrock, D. Dowson, “*Isothermal elastohydrodynamiclubrication of point contacts: Part I. Theoretical formulation*”, J. Lubr. Technol., 98, 2, pp. 223–229, 1976.
- [17] B.J. Hamrock, D. Dowson, “*Isothermal elastohydrodynamiclubrication of point contacts: Part II. Ellipticity parameter results*”, J. Lubr. Technol., 98, 3, pp. 375–383, 1976.
- [18] W.Z. Wang H. Chen, Y.Z. Hu, H. Wang, “*Effect of surface roughness parameters on mixed lubrication characteristics*”, Tribol. Int. Volume 39, Issue 6, Pages 522–527, 2006.
- [19] D. Zhu, “*Effect of surface roughness on mixed EHD lubrication characteristics*” Tribol Trans, 46, 1, pp. 44–48, 2003.
- [20] M. Kaneta, “*Effects of surface roughness in elastohydrodynamic lubrication*”, JSME International Journal, Series III (ISSN 0914-8825), vol. 35, no. 4, p. 535-546, 1992.

Appendix

Dimensional parameters

B = half width of hertzian contact zone $b = 4R\sqrt{\frac{W}{2\pi}}$ (m)

E' = effective elastic modulus of bodies 1 and 2 (Pa)

h = film thickness (m)

p = pressure (Pa)

p_h = maximum hertzian pressure $p_h = \frac{E'b}{4R}$ (Pa)

R = radius of contact (m)

u_m = average sliding speed (m/s)

w = applied load per unit length (N/m)

μ_o = inlet viscosity of the lubricant (Pa s)

ρ_o = inlet mass density of the lubricant (kg/m³)

μ = lubricant viscosity at the local pressure (Pa s)

ρ = lubricant mass density at the local pressure (kg/m³)

α = piezo-viscous coefficient (Pa⁻¹)

x = coordinate in the direction of surface velocity (m)

Dimensionless parameters

G = dimensionless load parameter $G = \alpha E'$

H = dimensionless film thickness $H = \frac{hR}{b^2}$

P = dimensionless pressure $P = \frac{p}{P_h}$

U = dimensionless speed parameter $U = \frac{\mu_o u_m}{E' R}$

W = dimensionless load parameter $W = \frac{w}{E' R}$

$\bar{\mu}$ = dimensionless viscosity $\bar{\mu} = \frac{\mu}{\mu_o}$

$\bar{\rho}$ = dimensionless mass density $\bar{\rho} = \frac{\rho}{\rho_o}$

Z = Roelands parameter

X = dimensionless coordinate in x direction $X = \frac{x}{b}$

B = Doolittle parameter

V_{occ} = occupied volume

V = volume

V_o = volume for $p=0$

K_0 = isotherm bulk modulus at $p=0$ (Pa)

K_0' = pressure rate of change of isothermal bulk modulus at $p=0$